A Novel Use of Negative Ion Mobility Spectrometry for Measuring Electron Attachment Rates

ARTICLE *in* THE JOURNAL OF PHYSICAL CHEMISTRY A · JULY 2004

Impact Factor: 2.69 · DOI: 10.1021/jp048809b

2 AUTHORS:

Mahmoud Tabrizchi
Isfahan University of Technology
72 PUBLICATIONS **798** CITATIONS

SEE PROFILE

Azra Abedi
Islamic Azad University
5 PUBLICATIONS **69** CITATIONS

SEE PROFILE

A Novel Use of Negative Ion Mobility Spectrometry for Measuring Electron Attachment Rates

Mahmoud Tabrizchi*,† and Azra Abedi

Chemistry Department, Isfahan University of Technology, Isfahan, 84154, Iran

Received: March 17, 2004; In Final Form: May 12, 2004

A new experimental approach based on swarm techniques was proposed for the measurement of rate constant of an electron attachment process at atmospheric pressure by means of negative ion mobility spectrometry. In this technique, sample is continuously delivered to the drift gas, which then enters into the drift region where it reacts with a counterflowing swarm of electrons injected by the shutter grid. As a result, negative ions are formed in the drift tube and a tail appears in the ion mobility spectrum. It is shown that the tail fits to an exponential function and the magnitude of the electron attachment rate constant value can be extracted from the plot of ln(ion intensity) versus the drift time. Unlike conventional electron swarm technique, it is not necessary, in this method, to perform the experiment at various concentrations of the sample. The approach proposed was typically examined for CCl_4, $CHCl_3$, and CH_2Cl_2 and the rate constants were estimated for a range of mean electron energies ($\langle\epsilon\rangle = 0.28-0.88$ eV) in nitrogen buffer gas at 300 K. Good agreement between the rate constant measured in the present work with those reported in earlier works is observed.

1. Introduction

Attachment of low-energy electrons to molecules in gas phase has been an active area of research from both experimental and theoretical points of view. These studies are important in various fields such as electric discharges, plasmas, lasers, and atmospheric chemistry. There are several experimental techniques which have been extensively used in studies of low-energy electron attachment. These include the high-Rydberg collisional ionization, rare-gas photoionization, crossed-beams, reversal electron attachment detector, the Cavalleri electron density sampling, electron swarm, flowing-afterglow/Langmuir-prob, and microwave conductivity/pulsed radiolysis techniques.[1,2] In most cases, electron attachment has been studied by negative ion mass spectrometry. In a few cases, however, it has been observed by means of ion mobility spectrometry (IMS). IMS is basically an ion separation technique at atmospheric pressure.[3,4] In this technique, ions are separated according to their individual velocities as they drift through an inert gas, driven by an electric field.[5−7] It is a simple, inexpensive, and sensitive analytical method for the detection of organic trace compounds.

Karasek et al.[8−10] have first proposed IMS as an efficient technique for the investigation of electron capture behavior of molecules. They reported experimental evidence of dissociative electron capture for halogenated aromatics with formation of a halogen ion as well as simple electron attachment for nitrobenzene with formation of a negative molecular ion.[10] Spangler and Lawless later measured the electron capture rate constant for chlorobenzene with an ion mobility spectrometer.[11] The procedure included the use of exponential dilution flask to vary the concentration of the sample introduced into the ionization region. Then, the rate constant was extracted from the plot of the number of Cl^- ions generated as a function of number of chlorobenzene molecules injected. Mayhew also used an ion mobility mass spectrometer to investigate the kinetics of low-energy electron attachment processes based on swarm techniques.[12−16] The major advantage of that instrument in comparison with a conventional electron swarm apparatus[17−19] was that the masses of the anion products resulting from the electron attachment process could be determined. The anion product masses are needed to investigate the electron attachment processes, however, other swarm techniques are not able to measure such values. Grimsrud et al. also measured thermal electron detachment of the molecular anion of azulene at elevated pressures by ion mobility spectrometry.[20] By this method, negative ions were introduced to a drift tube containing nitrogen gas. During the time required for an ion packet to drift, a portion of the ions undergo thermal electron detachment. From the IMS waveform thereby produced, the magnitude of the electron detachment rate constant value can be deduced.

In the conventional electron swarm technique, a pulsed swarm of electrons, produced at one end of a drift tube, is drawn under the influence of a uniform electric field through an inert buffer gas toward a collector at the other side of the tube. A small quantity (usually less than one part per million) of an attaching gas is added to the buffer gas. This results in removal of electrons and hence a reduction in the electron current. The amplitude of the electron pulse is then monitored as a function of the attaching gas concentration [*M*]. The density normalized electron attachment coefficient, α, can be extracted from the exponential attenuation equation:[16]

$$\frac{A}{A_o} = \exp(-\alpha L[M]) \tag{1}$$

where A and A_o are the pulse amplitude with and without attaching gas in the drift tube, respectively, and L is the length of the drift tube. The rate constant k is related to α by

$$k = w\alpha \tag{2}$$

where w is the electron drift velocity.

* Corresponding author. E-mail: m-tabriz@cc.iut.ac.ir.
† Regular Associate of the Abdus Salam ICTP.

10.1021/jp048809b CCC: $27.50
Published on Web 07/03/2004

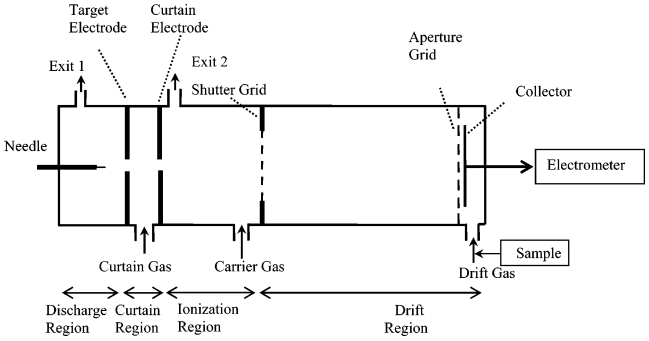

Figure 1. Schematic diagram of the negative corona discharge ion mobility spectrometer.

In the standard electron swarm technique, information is extracted from the reduction in the electron current. To use eq 1, it is necessary to perform the experiments at various sample concentrations [*M*], which is unfavorable because of time-consuming experimental measurements. In this paper, we describe a new method, using ion mobility spectrometry, for measuring electron attachment rate constants, in which the information is extracted from the negative ions. Unlike the electron swarm technique, it is sufficient, in this method, to perform the experiment at only a single concentration of sample.

2 Experimental Section

The ion mobility spectrometer used in this work was constructed in our laboratory at Isfahan University of Technology. A schematic diagram of the spectrometer is shown in Figure 1 and a detailed description of the instrument has been given in ref 21. The IMS cell is made of a glass tube, 4-cm inner diameter and 19-cm length, on which 15 stainless steel guard rings are mounted. The cell consists of four regions, namely, the discharge, the curtain, the ionization, and the drift region. Electrons are produced by the discharge between the needle and the target electrode which is a graphite disk with a small hole (1.5 mm) in its center. Electrons are then extracted by the second electrode (curtain electrode) into the ionization region and finally injected to the drift region by the shutter grid. A flow of dry nitrogen (about 120 mL/min) was introduced between the target and the curtain electrodes to prevent the diffusion of the sample into the discharge region. The sample can be introduced either into the ionization region via the carrier gas or into the drift region via the drift gas. The gas used in this work was pure nitrogen (99.9995%, Internmar B. V., Netherlands). Water vapor and other contaminations were removed by passing the gas through a 13*X* molecular sieves (Fluka) trap before entering the IMS cell. The flow rates of the carrier, the curtain, and the drift gases were about 100, 120, and 600 mL/min, respectively. The electric field strength in the drift region and the ionization region varied between 200−660 V/cm and a 100-μs pulse for shutter grid was typically used during the measurements. All experiments were performed at room temperature (300 K) and ambient pressure.

2.1. The Procedure. The method presented in this work is similar to the electron swarm technique. A swarm of electrons are allowed to enter a drift tube and move under the influence of a uniform electric field in an inert gas such as nitrogen. At the same time, a low concentration of an electron attaching substance is continuously delivered to the drift region. As the swarm travels within the buffer gas, electrons are captured by the electron-attaching molecules and negative ions are consequently generated in the drift region.

$$e + M \rightarrow M^- \tag{3}$$

The rate of the electron attachment reaction may be written as

$$\frac{\mathrm{d}[M^-]}{dt} = -\frac{d[e]}{dt} = k[M][e] \tag{4}$$

where [*e*] and [*M*] are the electron and the neutral electron attaching molecule concentrations, respectively. *k* is the electron attachment rate constant and *t* is the elapsed time. The neutral reactants, *M*, are present in great abundance compared to the electrons; thus, it is possible to assume that the sample concentration [*M*] is contant, and consequently, the reaction can be considered as a pseudo-first-order reaction. Then, the integration of eq 4 yields

$$\ln \frac{[e]_t}{[e]_o} = -k[M]t \tag{5}$$

where $[e]_o$ and $[e]_t$ are the initial concentration of electrons, and the electron concentration at elapsed time *t*, respectively. The elapsed time *t* may be substituted by $x = wt$, where *w* is the electron swarm velocity and *x* is the distance traveled by the swarm. The electron density at distance *x* from the injection point in the drift region will then be

$$[e]_x = [e]_o \exp\left(-\frac{k[M]x}{w}\right) \tag{6}$$

This equation shows that the electron swarm is exponentially diluted as it travels in the drift region.

The number of the negative ions formed at each point, *x*, of the drift region during the injection time of the electron swarm, t_g, can be calculated using eq 4.

$$[M^-] = \int_o^{t_g} k[M][e]dt \tag{7}$$

Since the concentration of electrons and neutrals are constant at each point, *x*, eq 7 is simplified to

$$[M^-]_x = k[M][e]_x t_g \tag{8}$$

Substitution of $[e]_x$ from eq 6 into eq 8 gives the distribution of the negative ions in the drift region.

$$[M^-]_x = k[M][e]_o t_g \exp\left(-\frac{k[M]x}{w}\right) \tag{9}$$

Generally, the speed of electrons is much higher than that of negative ions under the same conditions. For a typical value of $E/N = 15.5 \times 10^{-18}$ V cm^2 (commonly used in IMS), the electron velocity[22] is 5.29×10^5 cm s^{-1} while the ion velocities are about 10^3 cm s^{-1}. Thus, the negative ions do not move much during the short period of injecting electrons. In fact, a pulse of electrons flashes quickly through the drift tube and produces some negative ions that are distributed all along the drift tube on the basis of eq 9. Some negative ions are also formed in the ionization region, before the shutter grid. Those ions also pass through the shutter grid during the opening time along with the electrons. Therefore, a high concentration of negative ions exists near the shutter grid in addition to those produced by the electron swarm. Accordingly, the total distribution of the negative ions, immediately after opening the shutter grid, is predicted to be similar to that presented in Figure 2. The negative ions, then, drift all together with the same velocity toward the end of the

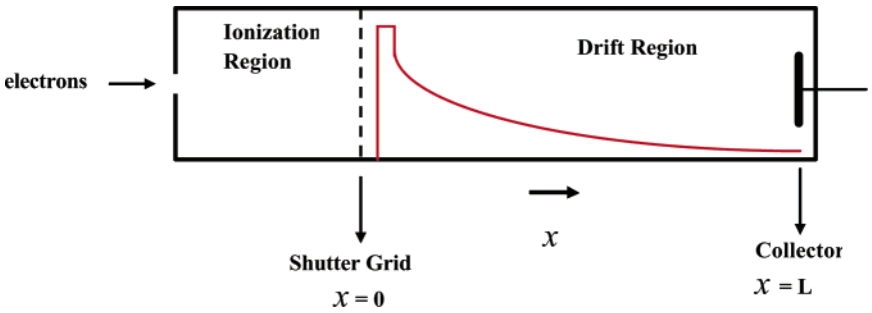

Figure 2. The distribution of the negative ions in the drift tube produced by an electron swarm.

drift tube. The waveform generated by the collector plate would be the mirror image of Figure 2, that is, a tail appears to the left of the negative ions peak. Each point, x, in the drift region corresponds to a point in the time domain. The point that shutter grid exists ($x = 0$) corresponds to t_p, the drift time of the negative ions peak. Therefore, x can be substituted by $x = v_d (t_p - t_d)$ where v_d is the drift velocity of the ion and t_d is the drifting time from the point x to the collector. Thus, the negative ion intensity, i, as a function of drift time for the tail would be

$$i \propto k [M][e]_o t_g \exp\left[-k[M]\frac{v_d}{w}(t_p - t_d)\right] \qquad (10)$$

This equation states that a plot of the logarithm of the ion current intensity versus drift time for the tail is a straight line with a slope proportional to the rate constant, k. If the drift velocity of the negative ions and the electrons as well as the sample concentration is known, the rate constant can then be easily determined.

2.2. Sample Introduction. The sample could be introduced either into the ionization region or into the drift region. In the first case, the drift region remained clean and no tail was observed in the ion mobility spectra. The tail was observed when the second setup was used. In this case, a low concentration of the sample was continuously delivered to the drift region. This was achieved by the insertion of a Swagelok T and a small glass vessel containing the sample into the source gas supply line leading to the drift region. The sample diffused to the drift gas via a fine capillary glass tube. The weight of the vessel was consecutively measured at constant temperature to obtain the flow rate of the sample and to calculate the sample concentration, [M], in the drift region. The sample concentration in all cases was more than 10^{-10} mol·L^{-1}. Considering the volume of the IMS cell, there would be about 2×10^{-11} mole sample in the drift region. The maximum electron current received at the collector in the absence of an electron-attaching sample was about 200 nA,[21] which is less than 2×10^{-16} mole electron in each 100-μs pulse. Therefore, the concentration of electrons was much less than that of the sample so that the sample concentration could be assumed to be constant during the reaction progress.

3. Results and Discussion

To practically evaluate the method, the rate constants for electron attachment reactions to CCl_4, $CHCl_3$, and CH_2Cl_2, as typical examples, were determined. It is well known that the electron attachment reaction to the aliphatic halides is a dissociative electron attachment reaction leading to the formation of a negative halide ion.[23]

$$RX + e \xrightarrow{k} RX^{-}* \xrightarrow{k^*} R + X^{-} \qquad (11)$$

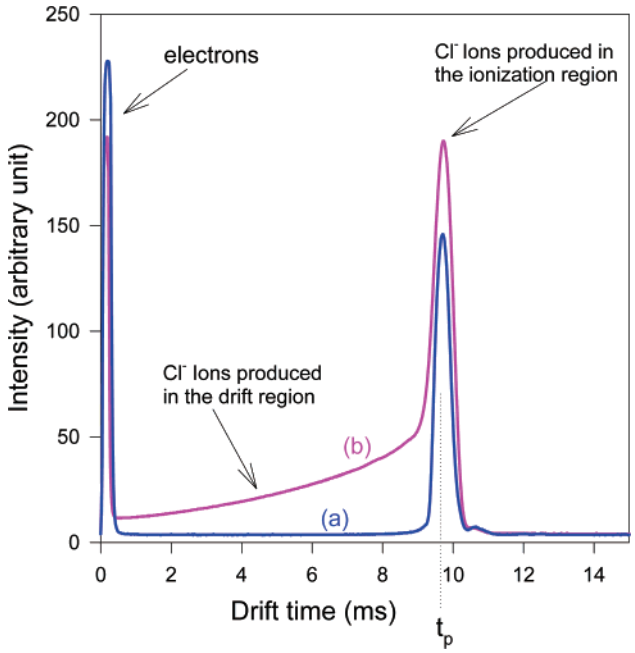

Figure 3. The ion mobility spectrum of CCl_4. (a) The sample was introduced into the ionization region and (b) the sample was introduced into the drift region.

Usually, the lifetime of RX^{-*} is very short (about 10−30 ps for CCl_4^-)[24] so that the reaction is controlled by the slow step of electron attachment reaction, k.

$$RX + e \xrightarrow{k} R + X^{-} \qquad (12)$$

3.1. CCl_4. The negative ion mobility spectrum of CCl_4 is shown in Figure 3. Trace a was recorded when CCl_4 was introduced into the ionization region. The peak near zero drift time corresponds to the electrons with very high mobility and the peak around 9.5 ms (t_p) corresponds to Cl^- ions. The background in trace a is almost zero and no tail is observed for the Cl^- peak. Trace b was recorded when the sample was introduced into the drift region. In trace b, again, the electrons and the Cl^- ions appear but the background is clearly not zero and a tail for Cl^- peak exists. The tail corresponds to the Cl^- ions that have been produced in the drift region. As expected, the spectrum is the mirror image of the negative ion distribution in the drift region, presented in Figure 2. The only remarkable difference is the presence of a peak at zero drift time. This peak corresponds to the electrons that could survive during the traveling of the swarm through the drift tube. On the basis of eq 10 if the natural logarithm of the ion intensity is plotted versus the drift time, the tail is expected to become a straight line. This is demonstrated in Figure 4b. The experiment was repeated at several drift fields and similar behavior was

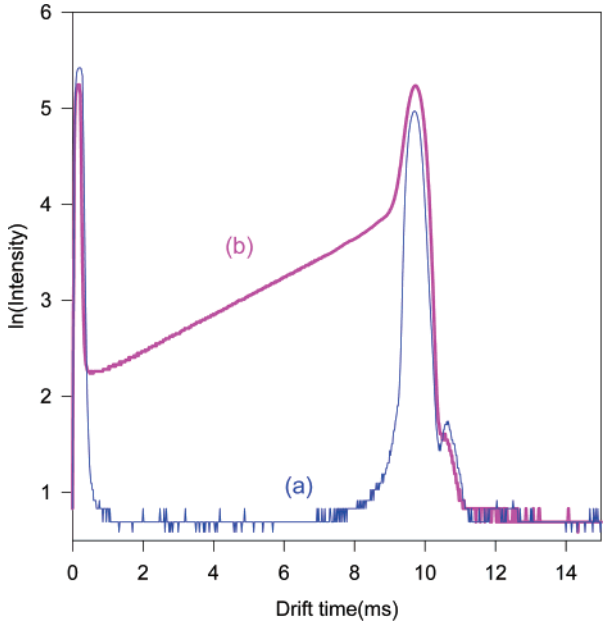

Figure 4. The plot of natural logarithm of the signal intensity versus the drift time. (a) The sample was introduced into the ionization region and (b) the sample was introduced into the drift region.

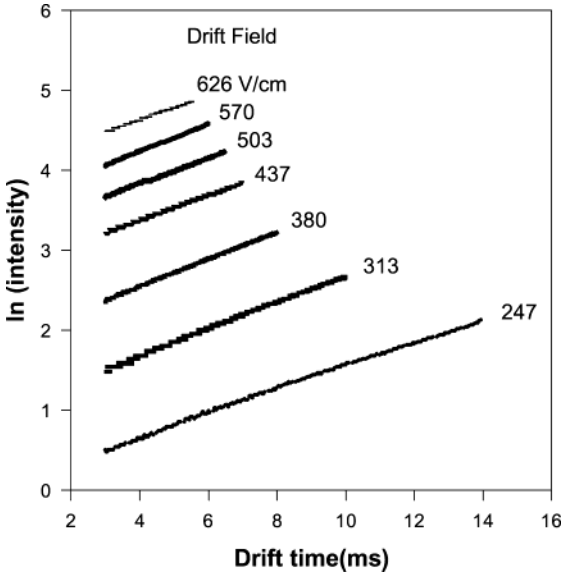

Figure 5. Logarithm of the signal intensity for the negative ion tail at various electric fields.

observed. The plots of logarithm of the tail versus drift time for various electric fields are presented in Figure 5. All plots are linear ($r^2 > 0.99$) and on the basis of eq 10 their slope would be $k[M]v_d/w$. To calculate the rate constant, the drift velocity of ions and electrons were required. The drift velocity of negative ions was calculated from the ion mobility spectrum using $v_d = L/t_p$ where L is the length of the drift tube and t_p is the drift time corresponding to the Cl^- ion peak. The electron drift velocity, w, depends on the value of E/N where E is the electric field and N is the neutral density in the drift region. The values for the electron velocity at each E/N were taken from ref 16. Finally, by measuring the concentration of the sample, the rate constant was calculated. The values of electron attachment rate constants measured for CCl_4 at various E/Ns are tabulated in Table 1. The values are not the same for all E/Ns since the electron attachment cross section depends on the kinetic energy of the electrons which is influenced by E/N.

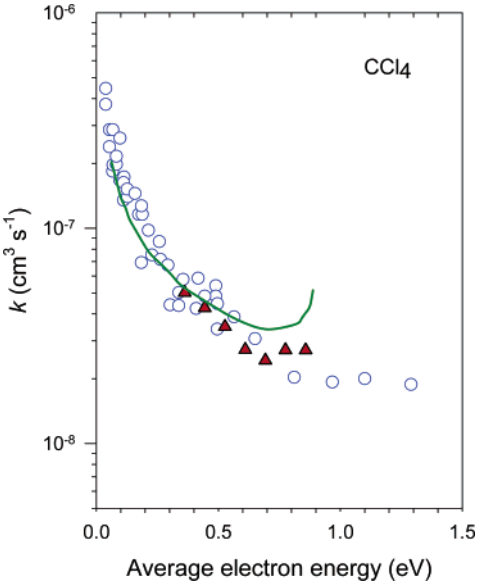

Figure 6. The electron attachment rate constant for CCl_4 in N_2 buffer gas at 300 K as a function of average electron energy. ▲ this work, ○ ref 26, and the solid line, ref 27.

TABLE 1: Electron Attachment Rate Constants, *k*, Obtained in This Work at Various *E*/*N*'S, and Different Electron Mean Energies, ⟨*e*⟩

	E/*N* ($/10^{-18}$ V·cm^2)	7.75	10.3	12.9	15.5	18.1	20.7	23.3	25.9
sample	⟨*e*⟩ (/eV)	0.28	0.36	0.44	0.53	0.61	0.69	0.78	0.88
CCl_4	*k* ($/10^{-8}$cm^{3}s^{-1})		5.02	4.26	3.49	2.73	2.45	2.72	2.72
$CHCl_3$	*k* ($/10^{-8}$cm^{3}s^{-1})	1.29	1.28	1.19	1.12	0.94	0.92	0.94	0.79
CH_2Cl_2	*k* ($/10^{-11}$cm^{3}s^{-1})	3.57	4.80	6.82	6.32	7.88	6.64	6.43	6.45

Electron attachment to CCl_4 is a dissociative reaction over the entire electron energies. There is a main peak at 0 eV and a small peak at 0.8 eV in electron attachment cross section curve of this molecule.[25] The values obtained in this work for electron attachment rate constants of CCl_4 have been compared in Figure 6 with other reported values. The results are clearly in good agreement with the reported data of Shimamori[26] and Christodoulides[27] obtained by the swarm technique. The mean electron energies at each E/N were taken from ref 22. It was not possible to extend the electron energy beyond 0.28−0.85 eV range since at the electric fields less than 200 V/cm the signal intensity was too weak to be used, and electric fields higher than 660 V/cm caused sparking.

3.2. $CHCl_3$. Electron attachment to chloroform has been studied by several research groups.[28,29,30] The electron attachment cross section for this molecule has two peaks at 0 and 0.3 eV[29] and Cl^- is the major ion below 1 eV.

$$CHCl_3 + e \rightarrow CH_2Cl + Cl^- \qquad (13)$$

The ion mobility spectrum of $CHCl_3$ is shown in Figure 7. Trace a was recorded when $CHCl_3$ was introduced into the ionization region while trace b was recorded when sample was introduced into the drift region. Again in trace b a tail for the Cl^- peak appears. Here, in trace b, unlike CCl_4, the Cl^- ion peak has shifted to longer drift times with respect to the peak in trace a. This was observed for any magnitude of the applied drift field. Although the two peaks arise from Cl^- ions, which is the result of the dissociation reaction 13, their drift times are not the same. The Cl^- ions that drift through the buffer gas, which contains a small amount of chloroform, arrive later than those drifting in pure buffer gas. The reason for this delay could be the

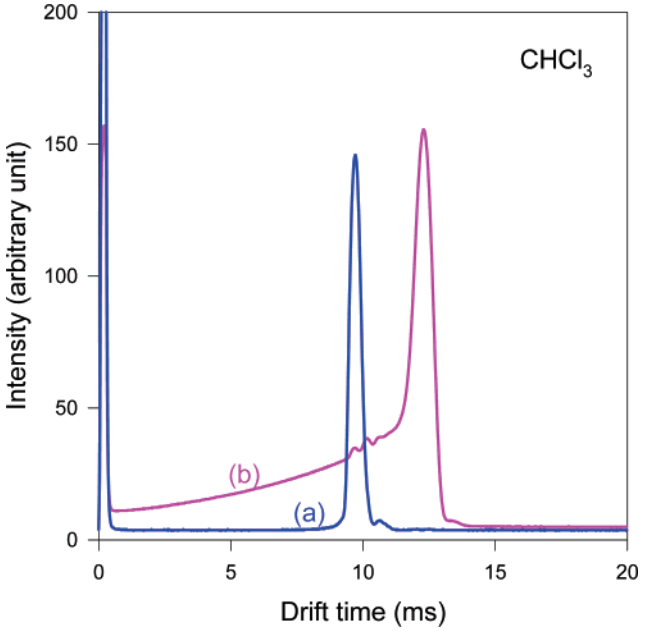

Figure 7. The ion mobility spectrum of $CHCl_3$. (a) The sample was introduced into the ionization region and (b) the sample was introduced into the drift region.

clustering of the negative ions with neutral chloroform molecules in the drift region. In general, ions in atmospheric pressure attach to neutral molecules such as the buffer gas or water vapor which is present in the buffer gas (reaction 14).

$$X^- + n(H_2O) \leftrightarrow X^-(H_2O)_n \quad (14)$$

If the sample concentration is high enough, the ions may even attach to the neutral sample molecules.

$$X^-(H_2O)_n + m(CH_3Cl) \leftrightarrow X^-(H_2O)_n(CH_3Cl)_m \quad (15)$$

However, if the sample is introduced only into the ionization region, there is no chloroform in the drift region and when ions enter that region, the equilibrium quickly moves back so that ions of the form $X^-(H_2O)_n$ reach the collector. In case b when the sample is introduced into the drift region equilibrium 15 continues all along the drift tube; thus, ions of the form $X^-(H_2O)_n(CH_3Cl)_m$ reach the collector. Apparently, the mobility of the later ions are less than that of $X^-(H_2O)_n$ ions. This results in a shift in the drift time of the negative ion peak for case b to longer drift times. The magnitude of the shift depends on the concentration of the sample in the drift region since a higher concentration of sample results in the formation of heavier clusters. This was practically confirmed by increasing the sample concentration and monitoring the magnitude of the shift. The shift also depends on the strength of the clustering which is a function of the ion−molecule interaction. Table 2 provides the thermodynamic data which demonstrate the relative strength of clustering of water and selected neutral molecules to Cl^- ions. The highest and the lowest equilibrium constants are those of $CHCl_3$ and CCl_4, respectively. The equilibrium constant for CCl_4 is 10^{-5} times as much as that of chloroform. That is why the shift was not observed for CCl_4. The shift was also observed, to a lesser extent, for CH_2Cl_2.

The clustering of ions or shifting the negative ion peak do not affect the rate constant extracted from eq 10, since the value of term $v_d(t_p - t_d)$ does not change by the clustering of ions. In fact, the clustering causes v_d to decrease but t_p and t_d to increase. This is clearer if v_d is substituted with d/t_p where d is the drift tube length. The term then becomes $d(t_p - t_d)/t_p$ which is invariant with respect to change in the drift times since the clustering increases both t_p and t_d with the same ratio.

TABLE 2: Thermodynamic Data for Clustering Reaction of Cl^- with Selected Neutral Molecules

reaction	$-\Delta_r H^0$ kcal mol^{-1}	$-\Delta_r S^0$ cal mol^{-1} K^{-1}	$-\Delta_r G^0$ kcal mol^{-1}	K_{eq}	ref
$Cl^- + H_2O \rightarrow Cl^-\cdot H_2O$	14.7 ± 0.6	19.7 ± 1.5	8.8	2.5×10^6	32
$Cl^- + CCl_4 \rightarrow Cl^-\cdot CCl_4$	13.4 ± 0.2	28 ± 3	5.0	4.4×10^3	33
$Cl^- + CHCl_3 \rightarrow Cl^-\cdot CHCl_3$	19.5 ± 0.2	25 ± 3	12	5.5×10^8	33
$Cl^- + CH_2Cl_2 \rightarrow Cl^-\cdot CH_2Cl_2$	14.8 ± 0.2	20 ± 3	8.8	2.6×10^6	33

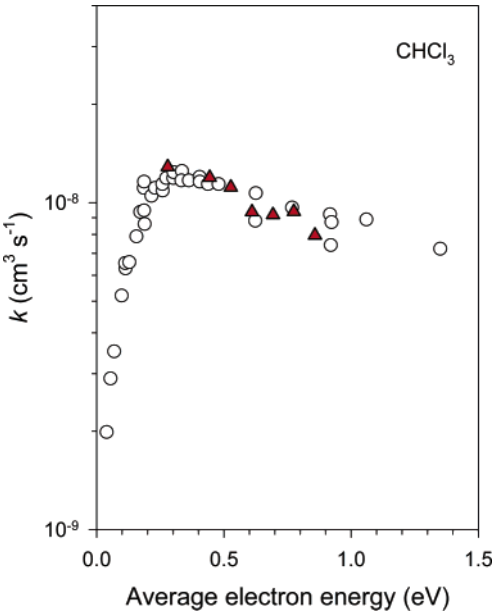

Figure 8. The electron attachment rate constant for $CHCl_3$ in N_2 buffer gas at 300 K as a function of average electron energy. ▲ this work, ○ ref 28.

As in CCl_4, the experiment was repeated at several drift fields to obtain the rate constant at various electron energies. The rate constants were derived from the slope of logarithm of the ion intensity versus the drift time. The values obtained for electron attachment rate constants at different average electron energies between 0.28 and 0.88 eV at 300 K are presented in Table 1. Figure 8 demonstrates that the results are in excellent agreement with those of Sunagawa et al.[28] obtained by the use of pulse-radiolysis microwave-cavity technique. There is a maximum for the rate constant around 0.3 eV which is in agreement with the presence of a peak in the cross section curve at about 0.3 eV.[29]

3.3. CH_2Cl_2. Electron attachment to CH_2Cl_2 is a dissociative reaction with a peak at about 0.7 eV in the cross section curve at 300 K.[31] The shift in the Cl^- ion peak was also observed for CH_2Cl_2 when the sample was introduced into the drift region. The magnitude of the shift was smaller than that of chloroform. This is expected from the thermodynamic data presented in Table 2. The equilibrium constant for the clustering reaction of CH_2Cl_2 is smaller than that for $CHCl_3$ but considerably larger than that for CCl_4. The described method was again used to measure the electron attachment rate constants for this molecule at various electron energies. The results are presented in Table 1 and Figure 9. Our results are in good agreement with the most recent data, measured by Pinnaduwage et all.[31] using high-temperature electron swarm technique.

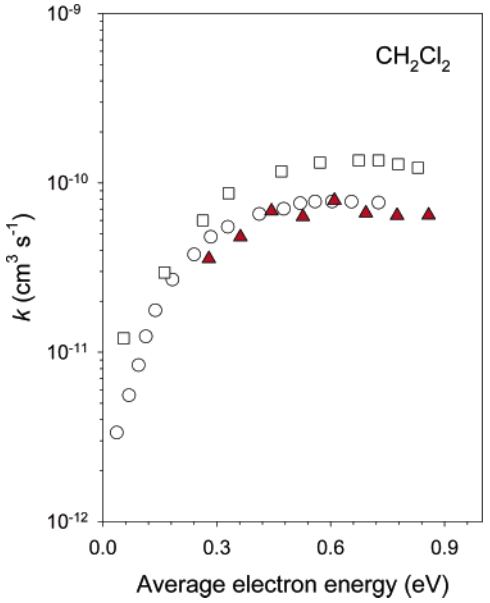

Figure 9. The electron attachment rate constant for CH_2Cl_2 in N_2 buffer gas at 300 K as a function of average electron energy. ▲ this work, ○ ref 31, and □ ref 27.

4. Conclusion

It was shown that the electron attachment rate constants can be successfully extracted from the tails in the negative ion mobility spectra when the sample is introduced in the drift region. The data obtained by this technique closely reproduce the reported data on the rate constants measured by other techniques. Since there is no need for vacuum in this technique, the use of IMS for such studies is simple, rapid, and inexpensive compared to other techniques. The technique can also be extended to the study of ion−molecule reaction rates at ambient pressure.

Acknowledgment. Authors would like to thank Dr. T. Khayamian and Prof. M. Amirnasr for valuable discussions. Financial support was provided by Isfahan University of Technology and the Center of Excellency in Chemistry. This work was presented in part at the 13th International Symposium on Electron-Molecule Collisions and Swarms, Pruhonice, Czech Republic, July 2003.

References and Notes

(1) Ingolfsson, O.; Weik, F.; Illenberger, E. *Int. J. Mass Spectrom. Ion Processes* **1996**, *155*, 1.
(2) Chutjian, A.; Garscadden, A.; Wadehra, J. M. *Phys. Rep.* **1996**, *264*, 393.
(3) Cohen, M. J.; Karasek, F. W. *J. Chromatogr. Sci.* **1970**, *8*, 330.
(4) Karasek, F. W. *Res. Dev.* **1970**, *21*, 34.
(5) Eiceman, G. A. *Ion Mobility Spectrometry*; CRC Press: Boca Raton, FL, 1993.
(6) Eiceman, G. A. *Crit. Rev. Anal. Chem.* **1991**, *22*, 17.
(7) St. Louis R. H.; Hill, H. H. *Crit. Rev. Anal. Chem.* **1990**, *m21*, 321.
(8) Karasek, F. W.; Spangler, G. E. Electron-capture process and ion mobility spectra in plasma chromatography. In *Plasma Chromatography*; Carr, T. W., Ed.; Plenum Press: New York, 1984; Chapter 15.
(9) Karasek, F. W.; Kane, D. M. *Anal. Chem.* **1973**, *45*, 576.
(10) Karasek, F. W.; Tatone, O. S.; Kane, D. M. *Anal. Chem.* **1973**, *45*, 1210.
(11) Spangler, G. E.; Lawless, P. A. *Anal. Chem.* **1978**, *50*, 290.
(12) Liu, Y.; Mayhew, C. A.; Peverall, R. *Int. J. Mass Spectrom. Ion Processes* **1996**, *152*, 225.
(13) Jarvis, G. K.; Peverall, R.; Mayhew, C. A. *J. Phys. B: At. Mol. Opt. Phys.* **1996**, *29*, L713.
(14) Jarvis, G. K.; Mayhew, C. A.; Singleton, L.; Spyrou, S. M. *Int. J. Mass Spectrom. Ion Processes* **1997**, *164*, 207.
(15) Jarvis, G. K.; Mayhew, C. A. *Int. J. Mass Spectrom.* **2001**, *206*, vii.
(16) Jarvis, G. K.; Kennedy, R. A.; Mayhew, C. A. *Int. J. Mass Spectrom.* **2001**, *205*, 253.
(17) Christophorou, L. G. *Atomic and molecular Radiation Physics*; Wiley-Intersience: New York, 1971.
(18) Hunter, S. R.; Christophorou, L. G. *J. Chem. Phys.* **1984**, *80*, 6150.
(19) Spyrou, S. M.; Christophorou, L. G. *J. Chem. Phys.* **1985**, *82*, 2620.
(20) Sahlstorm, K. E.; Knighton, W. B.; Grimsrud, E. P. *Int. J. Mass Spectrom.* **1998**, *179*/*180*, 117.
(21) Tabrizchi, M.; Abedi, A. *Int. J. Mass Spectrom.* **2002**, *218*, 75.
(22) Hunter, S. R.; Carter, J. G.; Christophorou, L. G. *J. Chem. Phys.* **1989**, *90*, 4879.
(23) Wentworth, W. E.; Becker, R. S.; Tung, R. *J. Phys. Chem.* **1967**, *71*, 1652.
(24) Kalamarides, A.; Marawar R. W.; Durham, M. A.; Lindsay, B. G.; Smith, K. A.; Dunning, F. B. *J. Chem. Phys.* **1990**, *93*, 4043.
(25) Matejcik, S.; Kiendler, A.; Stamatovic, A.; Märk, T. D. *Int. J. Mass Spectrom. Ion Processes* **1995**, *149*/*150*, 311.
(26) Shimamori, H.; Tatsumi, Y.; Ogawa, Y.; Sunagawa, T. *J. Chem. Phys.* **1992**, *97* (9), 6335.
(27) Christodoulides, A. A.; Christophorou, L. G. *J. Chem. Phys.* **1971**, *54*, 4691.
(28) Sunagawa, T.; Shimamori, H. *Int. J. Mass Spectrosc.* **2001**, *205*, 285.
(29) Matejcik, S.; Senn, G.; Scheier, P.; Kiendler, A.; Stamatovic, A.; Märk, T. D. *J. Chem. Phys.* **1997**, *107*, 8955.
(30) Skalny, J. D.; Matejcik, S.; Mikoviny, T.; Vencko, J.; Senn, G.; Stamatovic, A.; Mark T. D. *Int. J. Mass Spectrom.* **2001**, *205*, 77.
(31) Pinnaduwage, L. A.; Tav, C.; McCorkle, D. L.; Ding, W. X. *J. Chem. Phys.* **1999**, *110*, 9011.
(32) Hiraoka, K.; Mizuse, S.; Yamabe, S. *J. Phys. Chem.* **1988**, *92*, 3943.
(33) Hiraoka, K.; Mizuno, T.; Iino, T.; Eguchi, D. *J. Phys. Chem. A* **2001**, *105*, 4887.